

Strength of an Australian Coal Under Low Confinement

O. Buzzi · Y. Sieffert · J. Mendes · X. Liu ·
A. Giacomini · R. Seedsman

Received: 5 June 2013 / Accepted: 7 October 2013 / Published online: 20 October 2013
© Springer-Verlag Wien 2013

Keywords Coal · Brittle failure · Spalling · Soft rock

1 Introduction

Experimental testing of brittle rocks has shown that both brittle and ductile behaviours can be observed, depending on the level of confinement applied to the specimen. In particular, brittle rocks fail in a brittle mode as long as the confining stress falls below the Mogi line (Mogi 1966). Spalling of rocks is associated with brittle failure and is known to occur under low confinement, i.e. in the vicinity of excavation walls (Stacey 1981; Martin et al. 1999; Cai and Kaiser 2013). Indeed, at low confinement, large tension cracks may develop parallel to the excavation boundary when the stress exceeds the crack initiation threshold, which may lead to rapidly propagating instabilities and formation of thin slabs. Such slabs can represent a significant hazard to the workforce in confined mining excavations. Increasing the level of confinement modifies the nature and propagation mechanism of the cracks that develop upon loading: at high confinement, short shear

cracks develop and ultimately join to form a macroscopic shear band. Martin et al. (1999) showed that a single set of Hoek–Brown parameters failed to capture the two mechanisms and they distinguished Hoek–Brown frictional (for high confinement) and brittle (for low confinement) sets of parameters. Their proposed brittle criterion falls below the frictional counterpart reflecting a reduction in strength. Recently, Kaiser and Kim (2008) and Amann et al. (2012) proposed a non-convex criterion to capture the strength under both low and high confining pressures. However, some of the data they used involved a large degree of scatter (in Kaiser and Kim 2008) or not many points were obtained in the low confining range (in Amann et al. 2012). Considering the recent findings by Kaiser et al. and the lack of data in the literature about the strength of coal under low confinement, it has been decided to conduct a series of triaxial tests in order to mitigate this gap. Gaining a better understanding of the behaviour of the coal under low confinement is highly relevant for the stability of coal mine excavations.

2 Material and Specimens

2.1 Coal Origin and General Properties

The tests were performed on dull-banded coal (as per AS2519, Standards Association of Australia 1993) coming from the Mandalong mine, near Morisset (NSW, Australia). One coal block of about 20 kg that had fallen as a slab from a pillar rib was collected at a depth of approximately 250 m in the West Wallarah Seam. The West Wallarah Seam consists of massive coal plies with widely spaced bedding discontinuities; there is no apparent small-scale cleating within the plies, but there are joints extending

O. Buzzi (✉) · J. Mendes · X. Liu · A. Giacomini
Priority Research Centre for Geotechnical and Materials
Modelling, The University of Newcastle, Callaghan, NSW,
Australia
e-mail: Olivier.Buzzi@newcastle.edu.au

Y. Sieffert
Grenoble Université Joseph-Fourier, Laboratoire 3S-R, INP,
CNRS, B.P. 53X, 38041 Grenoble Cedex, France

R. Seedsman
Seedsman Geotechnics Pty Ltd, Mittagong, Australia

through the full seam thickness with spacings between wide and extremely wide. A typical proximate analysis indicates 18 % ash, 2.2 % moisture, 26.7 % volatile matter and 53.1 % fixed carbon. A typical maceral analysis gives 38 % of vitrinite, 4 % of liptinite and 52 % of inertinite (data supplied by Centennial Coal Company Limited, in accordance with AS2519). The density of solid particles was measured at 1.5 g/cm³ using an automated gas pycnometer (Autopyc from Micromeritics). Images obtained from thin sections microscopy clearly show the structure in fibres of the coal and some of the minerals and macerals (Fig. 1). The structure of the coal more resembles an interlocked crystalline rock with microcracks rather than a matrix supported porous sedimentary rock.

2.2 Coal Microstructure

Additional microstructural analyses were conducted in order to assess the possible degree of damage (i.e. microcracks) within the material. Five coal specimens, randomly taken from the same coal block, were subjected to the mercury intrusion porosimetry using an Autopore IV 9500 from Micromeritics. Figure 2 clearly shows the existence of small pores (below 1 µm, referred to as micropores) and,

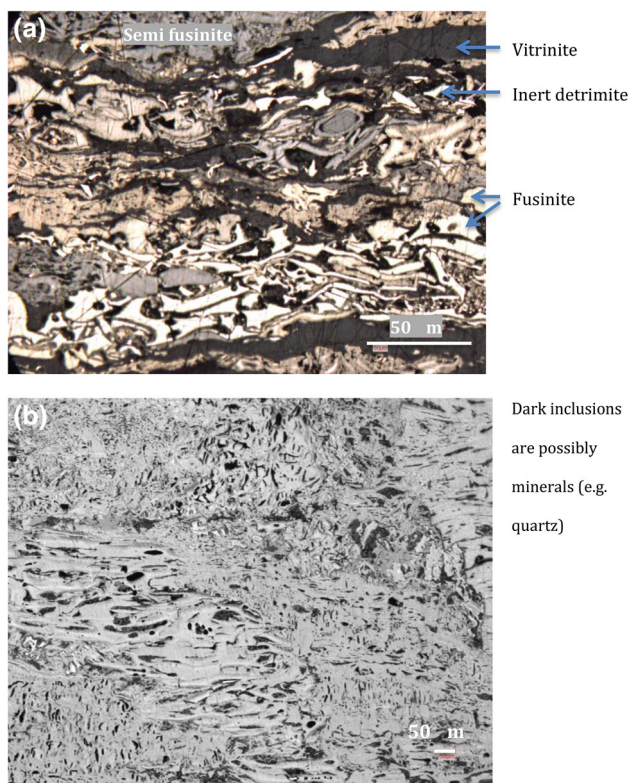


Fig. 1 Reflected light microscopy analysis (Zeissimage2) on thin sections of coal specimens. **a** Oil-immersion objective of magnification 50×. **b** Air Objective of magnification 10×

for four out of five samples, the presence of large pores (above 50 µm, referred to as macropores). Although the left side of the peak pertaining to micropores could not be fully ascertained (limitation of the Autopore pressure to 233 MPa), the two peaks are separated by two orders of magnitude in pore diameter.

Figure 2 is interesting since it highlights the natural variability of the material tested. In particular, the largest pores, representative of cracks, are variable both in dominant size (position of the peak) and corresponding density (height of the peak). At this stage, it is not possible to assess whether these cracks are inherent to the material, a consequence of the mechanical excavation process or due to the block falling from the pillar rib.

2.3 Coal Permeability

An attempt was made to measure the coal permeability using a classical approach of constant pressure gradients and water flow measurements, but this proved unsuccessful as the material permeability is very low (no flow was observed for a gradient of 4×10^3 m/m). As an alternative, the coal permeability was evaluated using the Katz Thompson model based on MIP data (Katz and Thompson 1986, 1987). The model was initially validated for sedimentary rocks and later on for cementitious materials (El-Dieb and Hooton 1994). The general formulation of the model is as follows:

$$K = c \cdot d_c \cdot d_{max} \cdot \phi \cdot S(d_{max}) \quad (1)$$

where K is the intrinsic permeability (in m²), ϕ is the maximum porosity intruded by mercury, c is a constant equal to 1/226, d_c is the critical pore diameter (inferred from MIP data), d_{max} is the characteristic dimension that

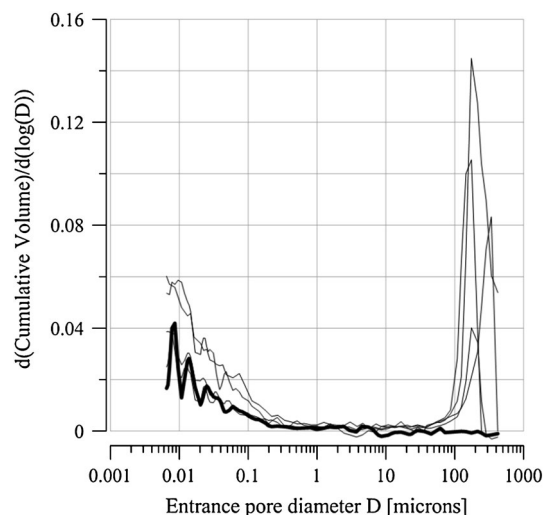


Fig. 2 Pore size distribution of five coal specimens taken randomly within the parent block

corresponds to the maximum conductance (inferred from MIP data) and $S(d_{\max})$ is the fractional volume of connected pore space involving pores larger or equal to d_{\max} (inferred from MIP data). For the sake of conciseness, the calculation of d_c , d_{\max} and $S(d_{\max})$ from pore size distribution is not detailed here. The reader is invited to refer to El-Dieb and Hooton (1994). The original model was developed for monomodal pore size distribution, but the coal tested herein has a bimodal distribution (Fig. 2).

The intrinsic permeability for the micropores was found to be in the order of 10^{-19} – 10^{-21} m² for the five coal specimens tested (d_c and d_{\max} < 10 nm) and around 10^{-12} m² for the macropores of four coals (d_c and d_{\max} in excess of 100 μm). Zheng et al. (1991) suggested that the macropores are critical when it comes to fluid flow in coal. However, the values of intrinsic permeability obtained by the model (10^{-12} m²) contradict the experimental observations (no flow). This might be explained by a limited connectivity of the macrocracks, which would impede water flow but not necessarily be picked up by MIP. Indeed, mercury intrudes the material from all outer faces, but does not require mercury flow across the specimen. In contrast, the permeability pertaining to the micropores is in agreement with the values obtained by Wang et al. (2013) on coal, and is considered to be more likely representative of the permeability of material herein tested.

2.4 Specimen Preparation

For the strength tests, specimens of small dimensions (12 mm diameter, 24 mm height) were used to limit the variability of the material and the presence of cleats within the specimens. The samples were cored with the stratification perpendicular to the long axis and were surfaced using a guiding system on a rotating grinding device. This ensured that the two faces were flat, parallel and perpendicular to the long axis in tolerances recommended by the International Society of Rock Mechanics (ISRM 1978).

Although a diameter of at least 54 mm is preferred for triaxial testing, the actual criterion ruling the minimum specimen diameter pertains to the ratio of diameter over maximum grain size, which must exceed 10 (ISRM 1978; ASTM D7012 2010). Note that, as far as we are aware, there is no specific standard dedicated to coal testing under triaxial conditions. Because of its nature, coal cannot be characterized by a particular grain size, i.e. it contains more macerals (fibres) than minerals (grains). However, the thin sections did not show any particles, inclusions or fibres larger than 1.2 mm and, hence, it was concluded that with a diameter of 12 mm, the condition of specimen homogeneity and representativity is satisfied.

The specimens were tested under the natural moisture conditions, i.e. as collected (Table 1). With little variation

Table 1 Specimens tested under triaxial conditions and their characteristics

Specimen #	Mass (g)	Density (g/cm ³)	W (%)	S_r	e
1	–	–	–	–	–
2	3.76	1.40	1.7	0.29	0.09
3	3.67	1.37	2.7	0.33	0.12
4	3.59	1.38	2.4	0.32	0.11
5	–	–	–	–	–
6	3.72	1.39	3.1	0.41	0.11
7	3.72	1.40	2.5	0.37	0.10
8	3.65	1.38	3.3	0.40	0.13
9	3.65	1.38	3.2	0.39	0.12
10	3.72	1.39	3.6	0.46	0.12
11	3.63	1.40	2.9	0.43	0.10
12	–	–	–	–	–
13	–	–	–	–	–
14	3.55	1.36	2.9	0.32	0.13
15	3.63	1.37	2.5	0.31	0.12
16	3.73	1.38	2.0	0.28	0.11
17	3.76	1.40	2.2	0.33	0.10
18	3.71	1.38	2.4	0.32	0.11
19	3.64	1.37	2.3	0.28	0.12
20	3.68	1.38	2.1	0.30	0.11
21	3.73	1.38	2.2	0.30	0.11
22	3.66	1.37	2.2	0.27	0.12
23	3.70	1.38	2.3	0.32	0.11
24	–	–	–	–	–
25	3.74	1.39	2.5	0.36	0.10
26	3.44	1.38	3.8	0.45	0.13

Saturation degree (S_r) and void ratio (e) calculated with a density of solid particles of 1.5 g/cm³. Water content was measured post-testing (tests under undrained conditions), but not measured for specimens #1, 5, 12, 13 and 24 because the membrane was punctured after specimen failure

in moisture content across the specimens (standard deviation of 0.5 %), it was considered that these were in similar hydraulic conditions (and hence suction) and that the test results are all comparable.

3 Testing Facility and Procedure

The tests were conducted with a Bishop and Wesley triaxial cell having a maximum confinement capacity of 2 MPa. The setup was slightly modified to account for the small specimen dimensions. In particular, instead of resting on the bottom platen, the specimen was linked to the top piston by the latex membrane and o-rings prior to testing in order to minimise the load eccentricity. Eccentricity on the bottom platen does not raise any issue as this latter is not allowed to pivot; the parasite moment being then taken by the system.

The decision on an adequate loading rate was made following a series of eight tests where the loading rate was progressively increased from 7×10^{-8} [approximately the value recommended by Brace, cited in Hoek (1968), for a granite] to $7 \times 10^{-6} \text{ s}^{-1}$ on both saturated and unsaturated specimens in order to investigate the influence of the loading rate on the strength. Considering the low material permeability, it is likely that, even for the slowest loading rate, the tests conditions were close to undrained.

Following the tests pertaining to loading rate, another 26 specimens were tested for strength under a range of confining pressure and under a loading rate of $7 \times 10^{-6} \text{ s}^{-1}$. Because of the non-saturation of the specimens; the pore pressure could not be measured.

4 Results and Discussion

4.1 Effect of Loading Rate

Bearing in mind the inherent variability of geological materials, Fig. 3 suggests that the loading rate has no consistent effect when testing the coal under natural moisture conditions (labelled as “unsaturated” in Fig. 3). However, for the saturated coal specimens, the strength was found to increase with the loading rate.

The effect of the loading has been discussed by several researchers but with variable findings: Lajtai et al. (1991) did not observe any effect of the loading rate for saturated brittle rocks, which was confirmed by Okubo et al. (2006) who worked on coal. However, these latter recognised that a loading rate dependence was possible for other coals. Kodama et al. (2003) found that increasing the loading rate on saturated samples of sandstone resulted in higher unconfined compressive strength, similar to the results herein presented.

Note that no water was detected in the porous stones post-testing, which is consistent with the low material permeability, confirming the undrained conditions of the test. Following this preliminary series of tests, it was decided to perform the remaining triaxial tests (on the unsaturated specimens) under a loading rate of $7 \times 10^{-6} \text{ s}^{-1}$.

4.2 Strength Under Low Confinement

Twenty-six triaxial tests were conducted with a confining pressure ranging from 0 to 2000 kPa. The objective of the testing was to ascertain the possible failure envelope of the material, especially in the low range of confining pressure. Post-mortem analysis of the specimens revealed three different failure modes: splitting, shear band or a combination of both (Fig. 4). The classification was done according to

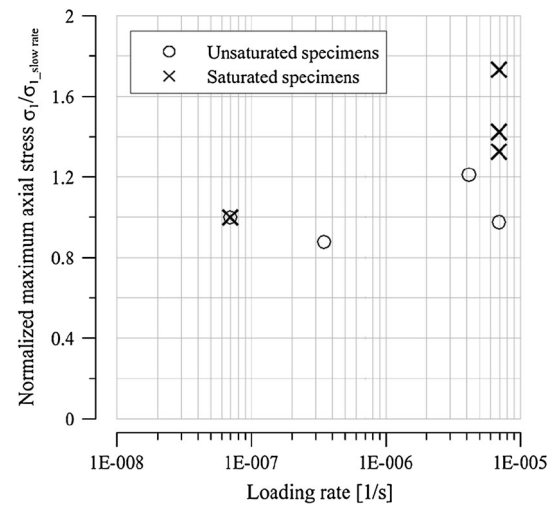


Fig. 3 Values of maximum axial stress (σ_1) normalized by the value obtained with the lowest loading rate ($\sigma_{1,slow}$) as a function of loading rate. Tests performed under 100 kPa of confinement with possibility for excess pore water to dissipate in the top and bottom porous stones, loading rate permitting. Average peak strength of unsaturated specimens at 35.2 MPa. Peak strength of saturated specimen at slowest loading: ≈ 31 MPa

the number and orientation of cracks as for most studies (Peng and Zhang 2007; Medhurst and Brown 1998; Amann et al. 2012). The decision to classify as “mixed” type of failure came when significant sub-vertical cracks developed in the half specimens on each side of the shear band.

Seventeen specimens failed by splitting, six failed with formation of a shear band (angle of the band from 60° to 75°) and three failed in a mixed mode. Medhurst and Brown (1998), among others, associate the failure pattern to the level of confinement. Here, at least 1200 kPa of confinement were required for a shear band to appear. However, after inspection of the shear band, it was found that the asperities had not been sheared off, suggesting that it is not truly a shearing mechanism but rather a tension crack.

Figure 5 shows the load–displacement curves for a selection of specimens (for clarity reasons). The response of the material appears to be brittle across the range of confinement tested, regardless of the failure mode. In addition, there is little influence of the confining pressure on the modulus of the material (except at no confinement). The initial nonlinear response (below 1 kN) for the lowest four curves is indicative of microcracks within the material, which is consistent with the findings of the MIP analysis.

Figure 6 shows the different values of peak axial stress plotted against the confining pressure. Unlike the results by Amann et al. (2012), quite a large number of data were obtained in the low confinement range and two zones can be identified. Up to 800 kPa of confinement, most of the

Fig. 4 Three types of failure modes observed. **a** Axial splitting, **b** shear band, **c** mixed axial splitting and shear band

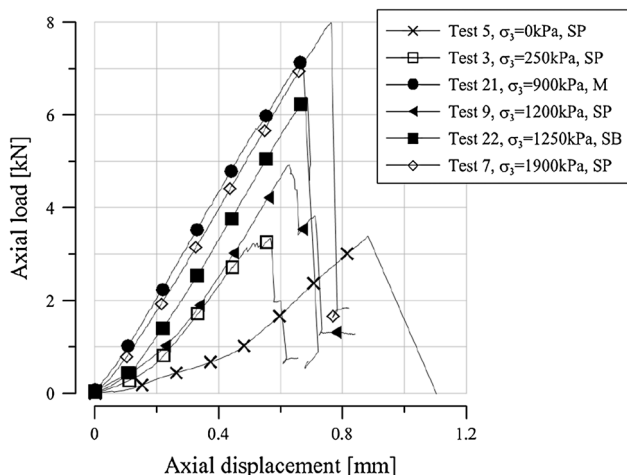
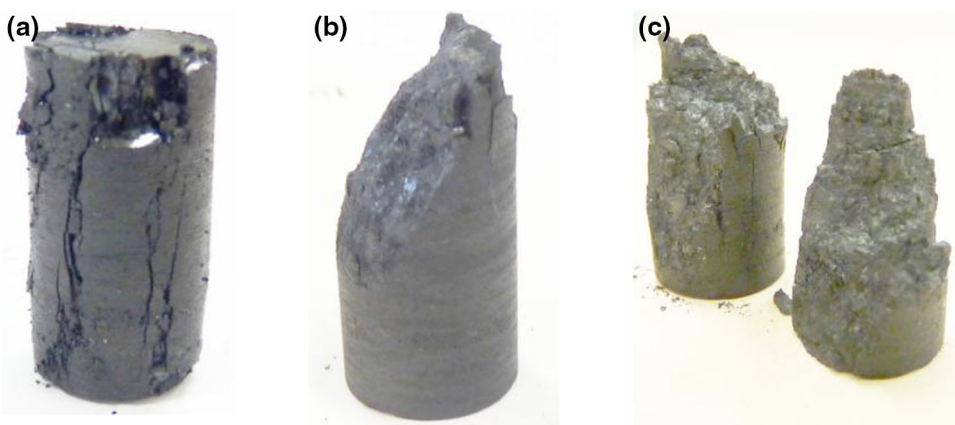


Fig. 5 Load–displacement curves for a selection of specimens. *SP* splitting, *SB* shear band, *M* mixed

specimens failed under an axial stress of about 30 MPa with little influence of the confining pressure. Only failure by splitting was observed in this range of confinement.

From 800 kPa, there is a clear effect of the confining pressure on the strength and in this zone the three types of failure are encountered. Some residual scattering can be observed in Fig. 6, which could be imputed to the natural variability of microstructure, as evidenced by the MIP analysis. The rest of the points appear to be falling along a line with a gradient of about 38. In their publications, Kaiser and Kim (2008) and Amann et al. (2012) clearly define a linear component in the failure criterion of intact brittle rocks, which they call the spalling limit. Based on their work, the line defined by $\sigma_1/\sigma_3 = 38$ could be seen as the material’s spalling limit of the coal tested.

The full S-shaped criterion proposed by Kaiser and Kim (2008) cannot be ascertained here. Indeed, this would require some tests under higher levels of confinement (at least higher than UCS/10 according to Amann et al. 2012), which is beyond the capacity of the current equipment.

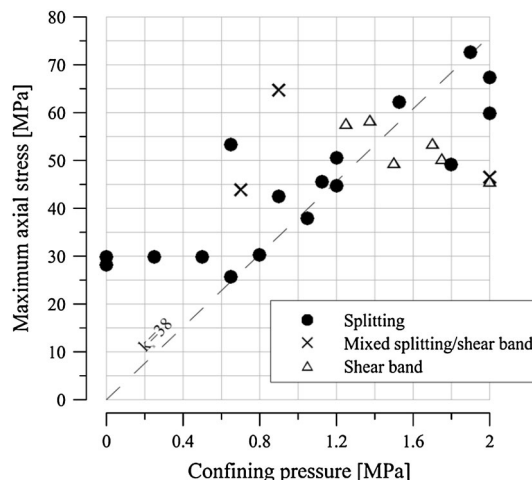


Fig. 6 Maximum axial stress (σ_1) versus confining pressure (σ_3) for all specimens

Still, the results clearly show a non-convex failure envelope for the intact coal used.

5 Conclusions

This paper presents the outcomes of a series of triaxial tests conducted on coal specimens coming from the West Wallarah seam, New South Wales, Australia. First, some tests showed that the loading rate, within the range considered, has little influence on the strength of the material when tested under natural moisture conditions. At least, no influence can be seen due to the natural variability of the material. Then, a series of compressions under triaxial conditions were performed with the objective to determine the failure envelope of the material. An appropriate number of tests were conducted in the region of low confining pressure and these clearly evidenced a non-convex failure criterion and a possible spalling limit, as defined by Kaiser and Kim (2008), of about 40. These results are consistent

with the findings by Amann et al. (2012) and provide new insight into the strength of coal under low confinement.

Acknowledgments The authors would like to thank Centennial Coal for having provided the coal specimens, Prof. Lanru Jing for fruitful scientific discussions and Seedsman Geotechnics Pty Ltd for funding part of this research. The help from Dr. Yanyan Sun in relation to thin section analysis is also gratefully acknowledged.

References

- Amann F, Kaiser P, Button EA (2012) Experimental study of brittle behavior of clay shale in rapid triaxial compression. *Rock Mech Rock Eng* 45:21–33
- ASTM Standard D7012–10 (2010) Standard test method for compressive strength and elastic moduli of intact rock core specimens under varying states of stress and temperatures. West Conshohocken, PA
- Cai M, Kaiser PK (2013) In-situ rock spalling strength near excavation boundaries. *Rock Mech. Rock Eng.* doi:10.1007/s00603-013-0437-0
- El-Dieb AS, Hooton RT (1994) Evaluation of the katz-thompson model for estimating the water permeability of cement-based materials from mercury intrusion porosimetry data. *Cem Concr Res* 24(3):443–455
- Hoek E (1968) Brittle fracture of rock. In: KG Stagg and OC Zienkiewicz (eds) *Rock mechanics in engineering practice*. Wiley, London, pp 99–124
- ISRM (1978) Suggested methods for determining the strength of rock materials in triaxial compression. *Int J Rock Mech Min Sci Geomech Abstr* 15:47–51
- Kaiser PK, Kim BH (2008) Rock mechanics advances of underground construction and mining. Keynote lecture, Korea Rock Mechanics Symposium, 2008, Seoul, pp 1–16
- Katz AJ, Thompson AH (1986) Quantitative prediction of permeability in porous rock. *Phys Rev B* 34(11):8179–8181
- Katz AJ and Thompson AH (1987) Prediction of rock electrical conductivity from mercury injection measurements. *J Geophys Res*, 92(B1):599–607
- Kodama N, Fujii Y, Ishijima Y (2003) The effect of temperature on the mechanical properties of Inada Granite and Shirahama sandstone. In: S Murata and T Saito (eds) *Proceedings of the 1st Kyoto international symposium on underground environment*, pp 187–195
- Lajtai EZ, Scott Duncan EJ, Carter BJ (1991) The effect of strain rate on rock strength. *Rock Mech Rock Eng* 24(2):99–109
- Martin CD, Kaiser PK, McCreath DR (1999) Hoek-Brown parameters for predixting the depth of brittle failure around tunnels. *Can Geotech J* 36:136–151
- Medhurst TP, Brown ET (1998) A study of the mechanical behaviour of coal for pillar design. *Int J Rock Mech Min Sci* 35(8):1087–1105
- Mogi K (1966) Pressure dependence of rock strength and transition from brittle fracture to ductile flow. *Bull Earthq Res Inst* 44:215–232
- Okubo S, Fukui K, Qingxin Q (2006) Uniaxial compression and tension tests of anthracite and loading rate dependence of peak strength. *Int J Coal Geol* 68:196–204
- Peng S, Zhang J (2007) *Engineering geology for underground rocks*. Springer, Berlin
- Stacey TR (1981) A simple extension strain criterion for fracture of brittle rock. *Int J Rock Mech Min Sci* 18:469–474
- Standards Association of Australia (1993) AS 2519 Guide to the Technical Evaluation of Higher Rank Coal Deposits, ISBN 0 7262 8114 X
- Wang S, Elsworth D, Jishan L (2013) Permeability evolution during progressive deformation of intact coal and implications for instability in underground coal seams. *Int J Rock Mech Min Sci* 58:34–45
- Zheng Z, Khodaverdian M, McLennan JD (1991) Static and dynamic testing of coal specimens. SCA Conference Paper Number 9120, Proceedings of the 1991 Society of Core Analysts 5th Ann. Tech. Conf., August 1991